

We are IntechOpen, the world's leading publisher of Open Access books Built by scientists, for scientists

6,900

Open access books available

186,000

International authors and editors

200M

Downloads

Our authors are among the

154

Countries delivered to

TOP 1%

most cited scientists

12.2%

Contributors from top 500 universities



WEB OF SCIENCE™

Selection of our books indexed in the Book Citation Index
in Web of Science™ Core Collection (BKCI)

Interested in publishing with us?
Contact book.department@intechopen.com

Numbers displayed above are based on latest data collected.
For more information visit www.intechopen.com



Effects of Interfacial Tension Alteration on the Destabilization of Water-Oil Emulsions

Aliyu Adebayo Sulaimon and
Bamikole Joshua Adeyemi

Additional information is available at the end of the chapter

<http://dx.doi.org/10.5772/intechopen.74769>

Abstract

Resolution of water-in-oil emulsion is a major crude oil processing requirement in oil industry. To improve the quality of the oil and fulfill regulatory requirements numerous chemical demulsifiers of varying efficiencies and effectiveness have been developed over the years. In this study, we have investigated the effects of water content, temperature, and different concentrations of Sodium Methyl Ester Sulfonate (*SMES*) on emulsion viscosity profiles and stability under distinct levels of salinities. The water content was measured with the American Standard Testing Method ASTM D4928 while SARA analysis was conducted using the ASTM D3279 and ASTM D6591 methods. The density and viscosity of the samples were measured following the ASTM D5002 and ASTM D445 techniques respectively while the emulsion stability was evaluated based on the rate of sedimentation, flocculation and coalescence from Turbiscan classic MA 2000. Refractometer with the aid of a light-emitting diode, a sapphire prism and a high-resolution optical sensor was used to measure the refractive index while interfacial tension was measured with spinning drop tensiometer. The emulsion samples were investigated at 25, 50 and 75°C. Analyses show that the interactions of the constituents of a crude oil system, the produced water system and the emulsion system play major roles in the characterization of water-in-crude oil emulsions. Hence, the stability of water-in-crude oil emulsions is related to the viscous force presented by the continuous phase, water cut and salinity.

Keywords: water-in-oil emulsion, sodium methyl ester sulfonate (*SMES*), demulsifier, Turbiscan MA 2000, ASTM D4928, ASTM D5002, ASTM D6591

1. Introduction

Crude oil is mostly produced as water-in-crude oil emulsion, carrying other dissolved and suspended organic and inorganic substances [1]. It is necessary to dehydrate crude oil before it is transported for refining [2, 3]. Crude oil emulsions are undesirable and can occur in nearly all stages of crude oil production, transport and refining [4, 5]. The emulsified water can occupy significant portions in the crude oil processing facilities, thereby increasing both capital and operating costs. Also, emulsions can lead to various changes in the characteristics and physical properties of the crude oils [6]. Dissolved and suspended materials such as salts, impurities, and finely divided solids, accompanied with produced water can lead to various problems during production and transportation of crude oils. These problems include pumping difficulty due to increased crude oil viscosity, corrosion of pipes and pumps, and poisoning of refinery catalysts [5, 7]. Also, sediments or solids in crude oil can cause equipment damaging, plugging, abrasion, erosion and residual product contamination [7]. Formation damage has also been reportedly caused by emulsions [8].

Pressure drops in flow lines can be high and sometimes cause trips and upsets of wet-crude oil handling equipment due to the presence of emulsified water, which may require an increase in the use of demulsifiers [4]. Unresolved emulsions can enter the oilfield environment, especially on offshore fields causing damage to aquatic lives. Besides, inefficiently dehydrated oil leads to revenue loss due to reduction in the quality of crude oil. Meanwhile, destabilizing water-in-crude oil emulsions remains a continuous challenge in the oil and gas industry due to the encapsulation of water droplets by rigid interfacial films. Understanding the materials responsible for the formation and stabilization of these emulsions is a key step towards efficient demulsification process [9, 10]. Therefore, the effect of water cut and salinity on emulsion resolution as the effect of temperature on interfacial film and the eventual droplet coalescence require detailed investigation. We hypothesize that the deformed interfacial film due to increase in temperature and presence of surfactant is regenerative thereby reducing the possibility of droplets coalescence and maintaining emulsion stability.

2. Emulsion formation and stabilization

Water-in-crude oil emulsions are formed due to high shear stresses at the flow restrictions such as choke valves and the wellhead during transportation of crude oil coupled with produced water [11, 12]. Water disperses in the crude oil forming droplets stabilized by the natural surfactants present in the later [13, 14]. Emulsion droplets undergo spherical to ellipsoidal shape deformation and subsequent break up to smaller drops during flow as shown in **Figure 1** [15, 16]. Droplet deformation is often resisted by the interfacial tension as determined by the Laplace pressure [17]. Thus, the following expression, that is, the capillary number (Ca) is used to determine the morphology of a droplet [15]:

$$Ca = \frac{n_o \dot{\gamma}}{\sigma/R} \quad (1)$$

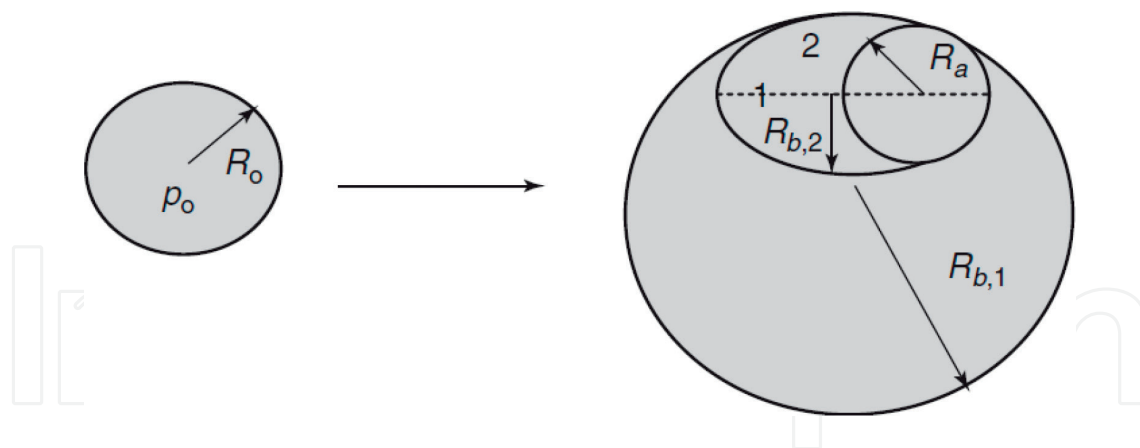


Figure 1. Illustration of increase in Laplace pressure when a spherical drop is deformed to a prolate ellipsoid [15].

where η_o is the viscosity of the medium, $\dot{\gamma}$ is the shear rate, σ is the interfacial tension, and R is the droplet radius.

In **Figure 1**, the radius of curvature (R_a) exists only near 1. However, two radii ($R_{b,1}$ and $R_{b,2}$) of curvature are present near 2. Therefore, smaller droplets require more stress to deform. Generally, the surrounding liquid transmits the needed stress through agitation. The magnitude of the transmitted stress depends on the level of agitation. Vigorous agitation will transmit high stress which will supply more energy to produce smaller drops. Emulsion formation is highly affected by the presence of surfactants in the system. Surfactants lower the interfacial tension and therefore the internal pressure leading to reduced stress required to break up a droplet. Surfactants also prevent new droplets from coalescing. Emulsification involves various processes such as droplet deformation, surfactant adsorption and droplet collision. These processes are illustrated in **Figure 2**. The thin lines depict the droplets while heavy lines and dots depict the surfactants.

Developing techniques for preventing and destabilizing crude oil emulsions requires adequate knowledge of the major properties of petroleum and the dispersed water which dictate the ultimate stability of the emulsion; the functional groups in the stabilizers which contribute to their interfacial activity; the interactions between the interfacially active components which are responsible for the stability of the emulsion [18, 19]. Asphaltenes have been reported to form aggregates which have an adsorbed covering sheath of aromatic resins as a stabilizing layer around dispersed water droplets in crude oil [11, 20–22].

Droplets in crude oil emulsions can be compared to colloidal particles in dispersion that frequently collide with each other which show that they are in Brownian motion. Hence, these droplets interact during such collision and this determines the stability of the system. The interactions can be in two forms which are attractive and repulsive. The droplets will coalesce and adhere together when the electrostatic dipole attraction between the water and oil molecules is high; however, the emulsion becomes stable if like charges exist as neighbors and the repulsive forces between the ions dominates [23]. Van der Waals forces constitute the main source of attraction between droplets or particles in colloidal systems since the particles are similar. Therefore, an emulsion can be said to be stable only if sufficient repulsion counteracts the attractive force between the droplets. The magnitude and range of only the van der Waals London

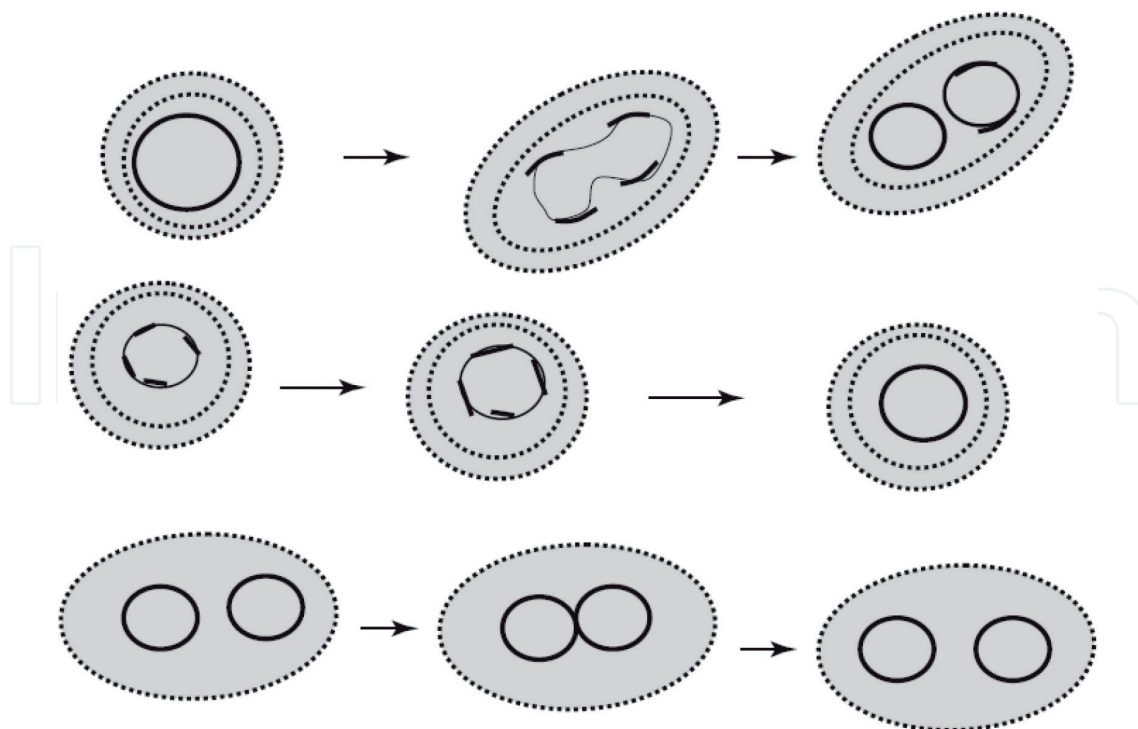


Figure 2. Schematic representation of the various processes occurring during emulsion formation [15].

(VDWL) attraction are the main determinants of how stable emulsion droplets can be due to the contribution of London forces to long-range attractions between emulsion droplets [24–26].

Coalescence occurs in three steps: (1) approach of the droplets through the continuous phase; (2) deformation of the droplets to form a thin film between them; and (3) thinning of this film to a critical thickness, below which the droplets coalesce [27, 28]. The suspension of droplets in a non-flowing continuous phase can be described as unsteady moving body in stationary fluid. The hydrodynamics of such droplets involves at least four forces: viscous force due to the viscosity of the continuous phase which describes the amount of friction between nearby regions of the fluid moving at different velocities; force of gravity which is a function of the composition of the droplets, force of attraction between the droplets (Van der Waal forces); and shearing forces which is the resultant of all the three forces [29]. Consequently, the hydrodynamics of emulsions lead to at least four mechanisms by which emulsions are stabilized. They are: Electrostatic repulsion; Steric repulsion; Thin film stabilization and; The Marangoni-Gibbs effect. In an emulsion stabilized with a surfactant, the homogeneous distribution of surfactant molecules on the surfaces of the drops is perturbed by the drainage of the liquid in the interfacial film [30]. The resulting non-homogeneous distribution of adsorbed surfactant molecules leads to the appearance of interfacial tension gradients. This non-equilibrium situation tends to be compensated by the migration of the surfactant molecules towards the interior of the interfacial film. This motion drags part of the liquid of the interface inside the interfacial film, producing a stabilizing effect that competes with the Van der Waals attraction between the drops surfaces. This work investigates the effect of interfacial tension alteration on the resolution of water-oil emulsions to pave way for formulation of environmentally friendly chemical demulsifiers.

3. Methodology

3.1. Material

The crude oil samples used for this research were obtained from PETRONAS, Melaka. The properties of the crude oil were determined according to standard procedures. Sodium Methyl Ester Sulfonate (*SMES*) is anionic surfactant produced by oil and fat obtained from green plants and animals. It has several properties which include good wetting ability, hard water resistance and softening, good solubility and highly degradable. It has also been used as an emulsifier with little stimulation to skin but high frothing ability. *SMES* has been synthesized from vegetable oil such as palm and jatropha oil [31]. Its toxicity and biodegradability have been tested [32, 33] and found to be comparatively better than most available anionic surfactants. Thus, *SMES* is well suited for environmentally friendly applications.

3.2. Water content measurement

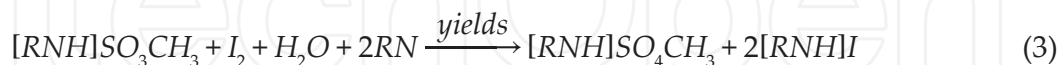
The water content of the crude oil was determined by standard test method. This measurement was necessary to ascertain the dryness of the crude oil and be able to correctly analyze any effects of water content on the stability and destabilization of its emulsions. Volumetric Karl Fischer titration (ASTM D4928) was used since water content in dry crude oil specification falls between 0.1 and 100%. The Karl Fischer (K-F) method is based on sulfur dioxide oxidation reaction by iodine in a methanoic hydroxide solution.

The two reactions involved in K-F titration are:

1. Where an alcohol (usually methanol or ethanol), sulfur dioxide (SO₂) and a base (RN) react to form an alkylsulfite intermediate:



2. Where the alkylsulfite reacts with iodine (I₂) and the water from the sample.



Since water and I₂ are consumed in equimolar amounts in reaction 2, if the amount of I₂ consumed is known, the amount of water that was present in the sample would be known.

3.3. SARA analysis

SARA analysis is important to determine the tendency of the crude oil to precipitate asphaltenes by calculating the asphaltene to resin (A/R) ratio, colloidal instability index (CII) and refractive index (RI) of the crude oil. The stability of resulting emulsions can also be estimated by applying the correlations among the various components of the crude oil. These determinants are necessary to study the behavior of the interfacial film between the crude oil and water droplets.

Asphaltene was removed by diluting the crude oil with n-heptane using a standard method prescribed in ASTM D3279 since asphaltenes are insoluble in liquid paraffins. The remaining components, saturates, aromatics and resins collectively known as maltenes are separated by polarities using ASTM D6591. The maltene with heptane was pumped through a chromatographic packed column of Agilent 1260 Infinity equipment for separation. The column contains silica and amine which have more affinity to more polar components. Resins which are the most polar of the maltenes are adsorbed on the column earlier thereby limiting heptane from pushing them through. Both the saturates and aromatics are pushed through the column by heptane but saturates would flow pass quicker due to their less polar nature. Thus, saturates are detected by the Refractive Index Detector (RID) of the equipment at a shorter time (retention time) than the aromatics which are more polar. The eluent (heptane) was replaced with Dichloromethane (DCM) to push out the resins using back flush since the resins are stuck near the top end of the column. Ultraviolet (UV) signals also record retention time for UV active components. In this case, only the aromatics are UV active and UV will only confirm the results of RID.

3.4. Density measurement

Density is a fundamental physical property that can be used in conjunction with other properties to characterize crude oil and other substances present in crude oil emulsions. It is useful when the hydrodynamics of emulsion droplets are discussed and can also help to investigate impact of particle collisions. Digital density analyzer was used to measure the densities in this study according to ASTM D5002. The density is measured with a U-shaped hollow glass tube, which is put into oscillation. The oscillation frequency of the tube filled with the sample is measured. The higher weight of the sample the lower the frequency. The density is calculated with the measured frequency. The density values of the crude oil, castor oil, fresh water, and two brine solutions (20 and 40 g/L) were obtained at room temperature, 50 and 70°C. Viscous force is an important phenomenon that prevents emulsion droplets from falling free when suspended in fluids. Standard method ASTM D445 was used to measure the viscosity of the crude oil. The EV 1000 instrument was used and it is based on a simple and reliable electromagnetic concept. Two coils move the piston back and forth magnetically at a constant force which could be likened to the movement of emulsion droplets under hydrodynamic and gravitational forces.

3.5. Refractive index and interfacial tension measurements

Dissolution of salts (e.g. NaCl) in water involves a process whereby Na^+ and Cl^- break free from the crystal-lattice structure of the solid. This process can be captured by examining the optical density of the aqueous solution. The index of refraction value of a material is a number that indicates the number of times slower that a light wave would be in that material than it is in a vacuum. A vacuum is given an n value of 1.0000. The n values of other materials are calculated from Eq. (4):

$$n_{\text{material}} = \frac{3.00 \times 10^8 \text{ m/s}}{V_{\text{material}}} \quad (4)$$

Refractometer with the aid of a light-emitting diode, a sapphire prism and a high-resolution optical sensor is used to measure the refractive index. The sample is put on the prism and

the measurement started. From a certain angle of incidence—the so-called critical angle—the ray no longer penetrates the sample but is fully reflected from its surface and is detected by the optical sensor. The refractive index is calculated from this critical angle. Emulsification is affected by interfacial tension and the separating potential between two or more phases. Interfacial tension is the work done to expand the interface between two non-mixing adjacent phases. At the separating boundary, the sum of cohesive forces is greater than the adhesive forces between the two phases. Accordingly, molecules at the interface have fewer attractive interacting partners than in the bulk phase. The phases therefore form the smallest possible interface without the action of external force.

Work must be done to expand the interface. Hence, cohesive and adhesive forces are critical to interfacial tension. The interfacial tension (IFT) of the crude oil in fresh water and the prepared brine solutions was determined using the spinning drop tensiometer. A horizontal capillary filled with a bulk phase and a drop phase is set in rotation. The diameter of the drop which is elongated by centrifugal force correlates with the interfacial tension. When a heavy bulk phase and a light drop phase are situated in a horizontal, rotating capillary, the drop radius perpendicular to the axis of rotation depends on the interfacial tension γ between the phases, the angular frequency ω of the rotation and the density difference $\Delta\rho$. Thus, with a given speed of rotation and with known densities of the two phases, the interfacial tension can be calculated from the measured drop diameter d ($=2r$) in accordance with Vonnegut's equation:

$$\gamma = \frac{r^3 \cdot \omega^2 \cdot \Delta\rho}{4} \quad (5)$$

3.6. Emulsion samples preparation

The kinetics of emulsion stability involves considerations on droplets interactions in the crude oil. The intra-actions within the droplets that are responsible for the droplets' momentum are also important. Thus, fresh water and brine solution formed droplets were examined in this study. Water-in-oil emulsions were prepared by mixing crude oil with fresh water and synthetic brine solutions in turn (volume/volume). Two brine solutions were prepared by diluting 20 grams and 40 grams of NaCl in a liter of distilled water to make 20 and 40 g/L aqueous solutions respectively. 20, 40 and 50 ml of fresh water were mixed with 80, 60 and 50 ml of crude oil respectively to make 20, 40 and 50% fresh water-in-crude oil emulsions. Similarly, 20, 40 and 50% brine-in-crude oil emulsions were prepared. These water cuts were chosen to capture the significance of droplets interactions in the crude oil since lower water cuts might defy resolution with the about-to-be tested demulsifiers. The two phases were homogenized using Hamilton constant mixer. No external emulsifier was used since the aim was to achieve natural emulsifier-stabilized emulsions. Agitation was allowed to take place for 5 minutes to achieve stable emulsions. About 100 ml of emulsion was prepared at a time for uniformity and repeatability purpose.

3.7. Emulsion stability measurement

Measuring the ability of a solution to conduct electric current is a crucial step in determining the presence of interfacial films especially when the phases involved have non-similar electrical conductivity values. Sulaimon and Bamikole [34] used the Turbiscan classic MA 2000 to

investigate the effect of stability on the aging of water-in-oil (w/o) emulsions for proper characterization and resolution. They concluded that the Turbiscan is a robust, accurate and automatic multiple light scattering technique for characterizing w/o emulsion stability. Through this method, the concentration of ions in brine solutions can be determined. The presence of interfacial films can easily be noted since crude oil does not conduct electricity. The effect of temperature on the conductivity of materials is significant. Conductivity measurements are taken at 25°C since the ionic activity increases with temperature. The electrical conductivity of the fresh water, two brine solutions, crude oil and the resulting emulsions were measured an electrical conductivity meter.

Measuring cylinders, 10 ml, were filled with emulsions and incubated in an oven at 25, 50 and 70°C for 5 days. Thereafter, the cylinders were removed, and the amount of separated water was recorded. This test was carried out using emulsions with all salinities and water cuts. Turbiscan classic MA 2000 was used to monitor the rate of sedimentation, flocculation and coalescence to determine the degree of stability of each emulsion composition formed. The testing tube was filled with 10 ml of emulsion and 10 acquisitions were made at room temperature. The autoscan was set to obtain a scan acquisition at every 2 minutes. Subsequently, the emulsions were heated to 50 and 70°C for 6 hours in a water bath and 10 acquisitions were also made at 2 minutes interval for comparison. Understanding the impact of collisions among emulsion droplets is important to study the destabilization of crude oil emulsions. Rotational viscometer was used to measure the deformation of the emulsion droplets under shearing forces. Rotational rheometry is most suited to very low shear rate / viscosity measurement, determining changes in structural properties via low amplitude and controlled strain oscillatory measurements. Double-gap plate was used since it has highest sensitivity for low viscous samples, lower inertia compared to other plates, nearly no impact on loading errors. The rheology was measured at 25, 50 and 70°C and the shear rate was varied from 1 to 1000 per second.

4. Results and discussion

4.1. Density and SARA analysis

The crude oil originally contained 0.2% water. This shows that the crude oil was within the specified limit of BS&W. Removing this intrinsic water content is difficult and may not be achieved with current dehydration techniques. Then, the crude oil (CO) was considered dry. The crude oil was then mixed with fresh water (SAL-0), 20,000 ppm aqueous solution of NaCl (SAL-1) and 40,000 ppm aqueous solution of NaCl (SAL-2) for this work. There exists a proportionate increase in density according to salt content in water as shown in **Table 1** since total pressure corresponds to the amount or number of particles present in the system. Solvation of NaCl crystal in water produced Na⁺ and Cl⁻(ions) surrounded by water molecules and the ions gained energy to move more freely. An increase in the number of salt particles led to more frequent collisions in the system. Obviously, fresh water has the lowest density while 40,000 ppm brine has the highest density. This observation can be explained by the amount of the average kinetic energy possessed by the particles in the liquids [35]. The particles in the crude oil gained more kinetic energy to move faster since there is no difficult barrier to

S/N	Temperature (°C)	Density (g/cc)			
		SAL-0	SAL-1	SAL-2	CRO
1	25	0.99704	1.0138	1.0258	0.9079
2	50	0.98803	1.0048	1.0163	0.8909
3	70	0.97776	0.9972	1.0083	0.8767

Table 1. Sample density.

overcome to do so. Perhaps, all the particles in the crude oil responded uniformly to temperature change. Dissociation of sodium chloride in water leads to encapsulation of Na⁺ and Cl⁻ in water molecules. Water molecules possess low kinetic energy and therefore prevented the salt ions from fully responding to temperature change. The ions, therefore, assumed the kinetic energy of the water molecules.

There was a corresponding decrease in viscosity with temperature due to easier movement of particles at elevated temperature. At low temperature, the particles are closely-packed, and their movement is restricted. Some components of the crude oil such as waxes are dissolved back into the bulk crude oil at higher temperature than their cloud points and thereby leaving other components which are resistant to heat such as asphaltene particles to move more freely. This phenomenon brings about easy flow of fluid and any other particle such as water droplets, introduced into the crude oil would move more freely and interact with the asphaltene particles. The SARA content of the crude oil is presented in **Table 2**. The crude oil contained 2.09% asphaltenes and 26.3% resins.

4.2. Effects of SMES on the intermolecular interactions and emulsion stability

Interfacial tension (IFT) of the crude oils SAL-0, SAL-1 and SAL-2 are presented in **Table 3**. Obviously, IFT decreases with temperature and it is highest in SAL-0 and lowest in SAL-1. Theoretically, IFT is a function of pressure, temperature and composition. The pressure exerted on the interfacial films was highest in SAL-1 and lowest in SAL-0 due to salt particles solvation forces acting in the aqueous solutions. The pressure is reduced in SAL-2 due to less collision impacts of the particles caused by incomplete solvation. Hence, the work required to break the interfacial films encapsulating resulting emulsion droplets would be highest for SAL-0 and least for SAL-1 droplets.

Component	Amount (%)
Asphaltene	2.09
Resin	26.30
Saturate	53.21
Aromatics	18.40

Table 2. SARA content of the crude oil.

Temp (°C)	IFT (mN/m)		
	Crude oil		
	SAL-0	SAL-1	SAL-2
50	13.9248	9.3770	11.6847
70	9.2829	5.3807	8.7446

Table 3. Interfacial tension of the crude oil.

The cohesive forces among molecules of fresh water are strong since there is no presence foreign material present. Fresh water tends to maintain a surface area that is as small as possible when in contact with crude oil due to their immiscibility and an interfacial tension will be maintained between the two liquids. Owing to the presence of the “surface active” component (asphaltenes) in the crude oil, its molecules will tend to be oriented between the two faces with the polar ends in the polar phase and the non-polar ends in the non-polar phase, which will lower interfacial tension.

The cohesion between the water molecules reduces when NaCl is introduced due to the solvation process. Both Na⁺ and Cl⁻ are surrounded by water molecules and thereby causing the molecules to move faster and collide more freely with the wall of the container. The pressure generated due to collisions leads to the tendency of SAL-1 maintaining lower IFT than fresh water. However, increase the salinity leads to higher adhesive forces among the particles of the salt and water molecules. The molecules are more packed in SAL-2 due to more NaCl molecules compared to the particles in SAL-1. Thus, more particles led to closer packing and lesser particle movement and collision since the particles tend towards the water molecules for solvation. Lesser pressure is therefore mounted on the wall of the container which resulted in higher IFT for SAL-2 as against that of SAL-1. Meanwhile, the IFT of SAL-0 is the highest since the cohesive forces in SAL-0 is greater than the adhesive forces in both SAL-1 and SAL-2. There was a great reduction in the IFT's when 50,000 and 150,000 ppm of Sodium Methyl-Ester Sulfonate (*SMES*) were added to the crude oil. However, SAL-1 droplets had higher IFT than SAL-2. At 50000 ppm shown in **Figure 3**, higher temperature (70°C) led to higher IFT of the mix in SAL-0 and SAL-2. This phenomenon was reversed when 150,000 ppm of *SMES* was added to the crude oil (**Figure 4**). The IFT of the crude in SAL-1 became higher at 70°C.

SMES preferentially migrated to the interface and caused lower IFT since it has more affinity to water molecules than the polar components of the crude oil. This follows the work of [36] where it was confirmed that demulsifiers are interfacially active and thus, replace weakly adsorbed natural emulsifiers. Subsequently, the droplets gained energy and interacted with the particles in the crude oil when the temperature was raised. The *SMES* molecules exhausted and thereby supported by the polar components of the crude oil. The effect of temperature was significant in SAL-1 since its initial momentum allowed it used up all the *SMES* molecules and attracted the polar components. Therefore, temperature effect dominated the events at 70°C. Increase in the concentration of *SMES* in the system prevented the polar components from taking significant impact in the interactions. However, dissolution of *SMES* was faster

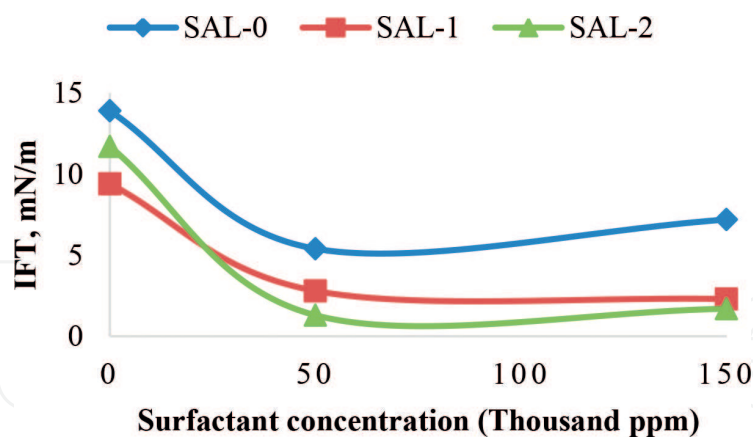


Figure 3. Critical micelle concentration of SMES at 50°C.

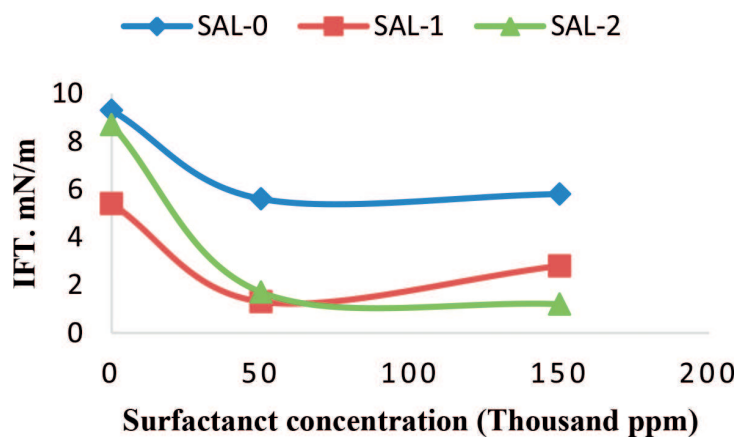


Figure 4. Critical micelle concentration of SMES at 70°C.

in SAL-1 due to agitation and thereby leading to higher IFT at 70°C since the interfacial film was made up of more polar components in the crude oil. The critical micelle concentration is approximately 60,000 ppm irrespective of salinity and temperature.

Three important properties of the emulsions formed were determined to gain insight into their behavior under different conditions. They are described in the following subsections. **Table 4** presents the electrical conductivities of the crude oil, SAL-0, SAL-1, SAL-2 and those of the resulting emulsions. The results show that electrical conductivity increased with salinity. The zero conductivity of the emulsions is an indication that the electrode of the conductivity meter could only contact the continuous phase and thereby giving the electrical conductivity of the crude oil as that of the emulsions. Hence, the SAL-0, SAL-1 and SAL-2 droplets were encapsulated by the natural emulsifiers in the crude oil. Interfacial films were therefore, confirmed to be present and all the emulsions formed were water-in-oil.

The kinetics of emulsion stability was studied by monitoring the behavior of the emulsions under the three different destabilization mechanisms: coalescence, flocculation, sedimentation. The following sub-subsections describe the results. Bottle tests gave no visible phase

Material	Electrical conductivity ($\mu\text{S/cm}$)
Crude oil	0
SAL-0	0.23
SAL-1	844
SAL-2	1665
All emulsions	0

Table 4. Electrical conductivity.

separation after the test period (5 days). Opacity was the only justification possible from the bottle tests to show that no coalescence occurred. This observation was common to all the emulsions formed and tested. While it was correct to ascertain that the emulsions were all stable due to absence of coalescence, there was no evidence to show there was no sedimentation and flocculation of the droplets. There was zero percent transmission for the entire column of the testing tube occupied by the emulsions. Zero transmission was an indication of opacity of the emulsions which confirmed the results obtained from the bottle tests. Back scattering profiles were then used for stability analysis.

The stability profiles of the emulsions were obtained for water-in-crude oil emulsions formed with SAL-0, SAL-1 and SAL-2 at 20, 40 and 50% water cuts i.e. SAL-0E20, SAL-0E40, SAL-0E50, SAL-1E20, SAL-1E40, SAL-1E50, SAL-2E20, SAL-2E40 and SAL-E50. All the emulsions were kinetically stable since the droplets remained highly dispersed and no appreciable change over an extended period. The droplets dispersed in an equilibrium manner. Thus, the repulsive forces impeding the aggregation of the emulsion droplets were sufficiently high. Elevated temperature reduced the continuous phase viscosity and enhanced force of gravity to dominate the stability process through sedimentation. The attractive forces between emulsion droplets might lead to constantly structured arrangement with stable phase. There was no observed cohesion of droplets (flocculation) in the tested emulsions. Flocculation might lead to bigger droplets which would facilitate sedimentation and disrupt phase stability leading to subsequent coalescence. Hence, aggregative stability was observed due to the ability of the emulsions to maintain the dispersion and segregation of the droplets. In aggregates, despite mobility alteration, the droplets probably remained as such for a period after which they could fuse extemporaneously with weakening phase interfacial capacity if destabilization techniques are applied. The Coalescence, that is, merging of droplets never occurred in any of the emulsions tested.

Crude oil is a Newtonian fluid as shown in the measured shear stress against shear rate. Approximately, its viscosity decreases with temperature but remains constant with shear rate. **Figures 5–7** show the rheology profiles of the crude oil (CRO) and effects of water cuts on the rheological behavior of the crude oil. It is shown that the water cuts change the rheological properties of crude oil by deviating from Newtonian fluid to non-Newtonian depending on the amount of water present in it. Emulsions are pseudo plastic or shear-thinning fluids. They have lower apparent viscosity at higher shear rates. According to Chhabra [37], pseudo plastic fluid is generally supposed that the large molecular chains tumble at random and affect large

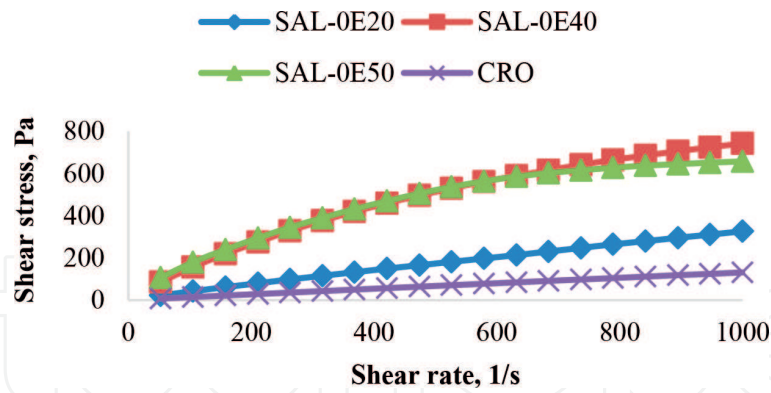


Figure 5. Rheological profile of fresh water-crude oil emulsions at 25°C.

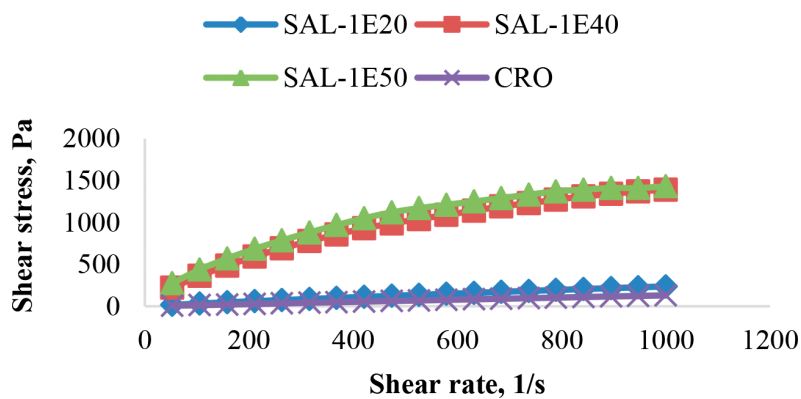


Figure 6. Rheological profile of brine (20 g/L salinity)-crude oil emulsions at 25°C.

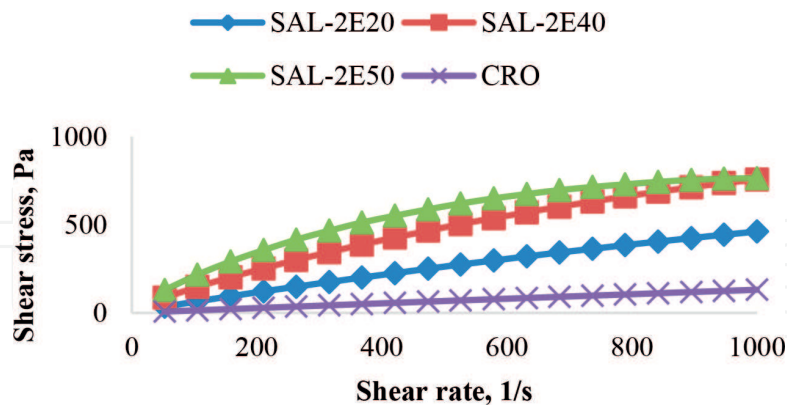


Figure 7. Rheological profile of brine (40 g/L salinity)-crude oil emulsions at 25°C.

volumes of fluid under low shear, but that they gradually align themselves in the direction of increasing shear and produce less resistance.

The effect of salinity on the rheological behavior exhibited by the emulsions is shown in **Figures 8–10**. Shear stress became highest on the emulsions of SAL-1 at higher water cuts. This behavior can be explained by considering the impact of droplet collisions with the emulsions.

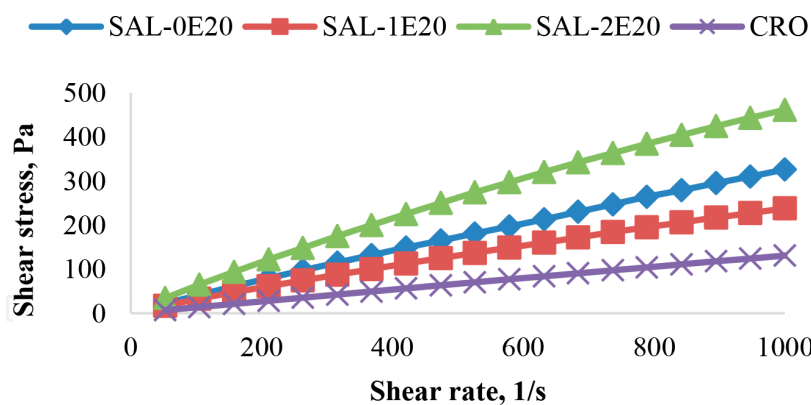


Figure 8. Rheological behavior of emulsions with 20% water cut at 25°C.

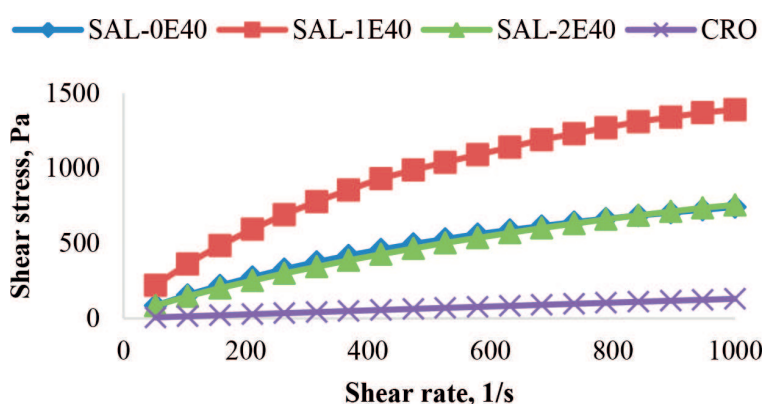


Figure 9. Rheological behavior of emulsions with 40% water cut at 25°C.

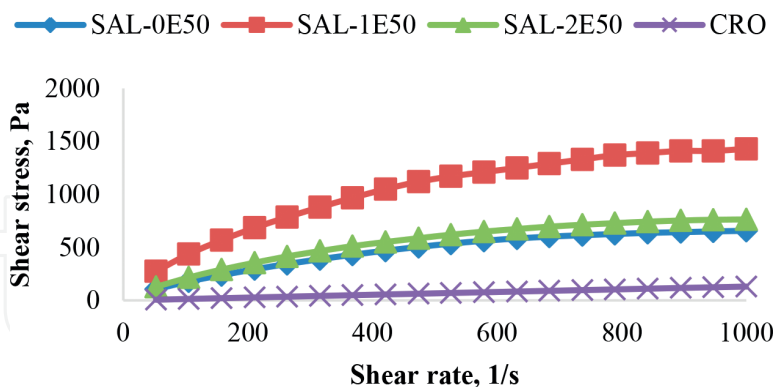


Figure 10. Rheological behavior of emulsions with 50% water cut at 25°C.

The amount of shear stress developed was dependent on the average kinetic energy of such droplets. At higher water cuts (40 and 50%), SAL-1 emulsions contained freer droplets that collide faster with higher impact due to shorter distance between the droplets. At lower water cut (20%), the viscous force within the continuous phase restricted the collision impact.

Figure 11 shows the changes in viscosity with shear rate at 70°C and different temperature and brine salinity for emulsions with 20% water cut. All the emulsions were non-Newtonian at room

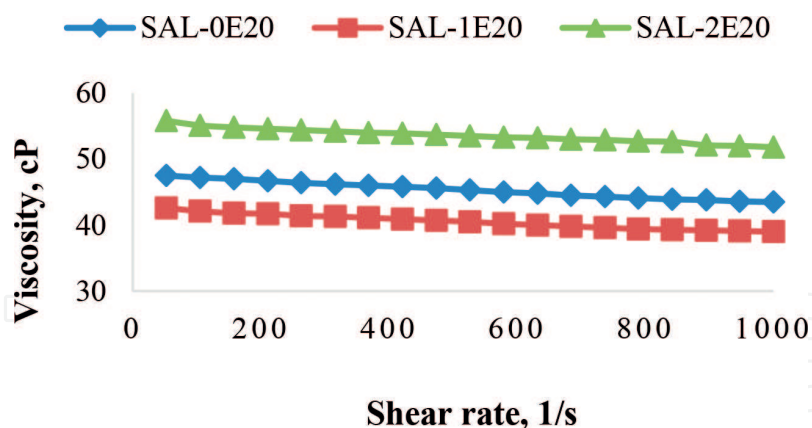


Figure 11. Rheological behavior of emulsions with 20% water cut at 70°C.

temperature irrespective of salinity. Obviously, SAL-2E20 was most viscous but the viscosity dropped fastest with shear rate. Droplets of SAL-2E20 contained ions that were more closely packed than those in SAL-1 droplets and required more work to break them. Also, SAL-0 droplets possess greater cohesive forces than the adhesive forces of SAL-1. Corresponding amount of energy was required to overcome these binding forces within the emulsion droplets. At increased shear rate, the frequency at which the droplets collided with each other and with the wall of their container increased. Denser droplets broke more often than less dense ones due to the intensity of the collision impact. The slopes of the rheology profile assumed approximately equal and constant values at elevated temperature since all droplets had reached the minimum size that could be broken by the shearing forces. Thus, the emulsions tend to assume the Newtonian behavior of the continuous phase.

The frequency of droplet collisions increased at 40% water cut due to a reduction in the distance between the droplets and therefore, leading to greater impact. The closeness of the droplets was responsible for the higher amount of shearing force required to overcome the resistance to flow of the emulsions. Hence, all the emulsions became more viscous than the emulsions at 20% water cut as shown in **Figure 12**. Droplet breakage occurred according to the molecular packing of the salt particles and water molecules. Droplets of SAL-2E40 broke fastest at lesser force due to highest density and collision impact. However, the slope of SAL-1E40 plot was higher due to high rate of deformation since the first collision impact. Emulsions with SAL-0E40 and SAL-2E40 required equal amount of energy to flow at the beginning of the shearing process. They had equal viscosity of 1630 cP each at 52500001/s due to similar collision intensity. However, they had unequal slope which eventually led to different but close viscosity values of 742 cP and 756 cP at 1000 1/s respectively. SAL-2E40 droplets broke down quicker since the product of the binding forces within SAL-2E40 was lesser than that in SAL-0E40. The droplets continued to break until the critical breaking size was achieved and the shearing force equaled to that required by the original crude oil. Thus, the emulsions tend to assume Newtonian behavior with shear rate and temperature.

The viscosity versus shear rate profiles of the emulsions at 50% water cut at the three test temperatures are shown in **Figure 13**. Increased water cut led to reduction in the distance between the droplets and thus, required greater shearing force. Further reduction in the

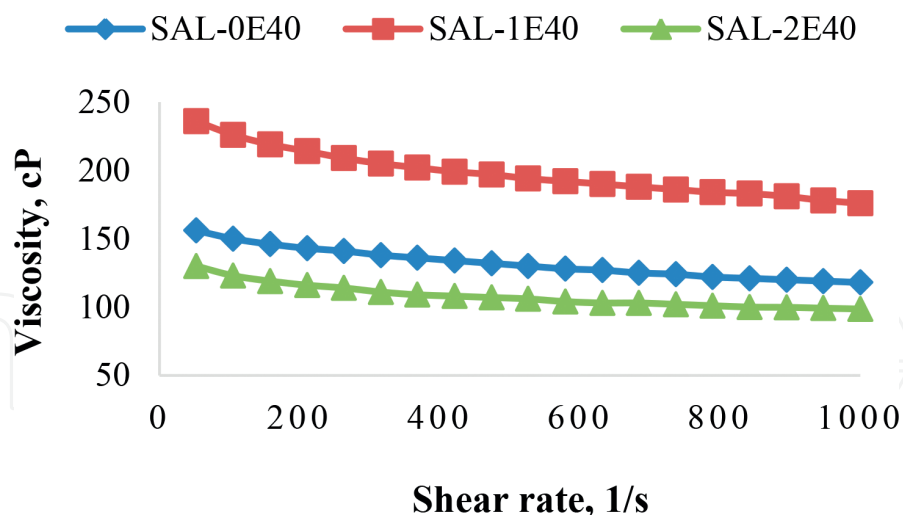


Figure 12. Rheological behavior of emulsions with 40% water cut at 70°C.

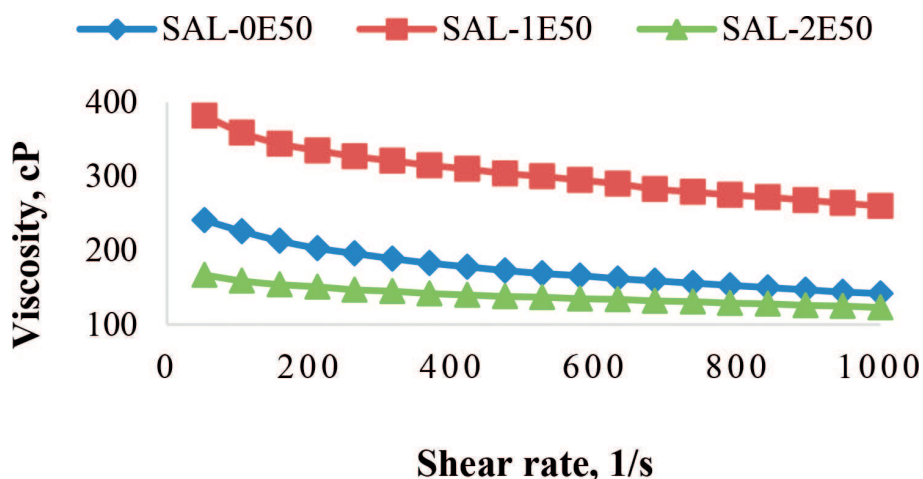


Figure 13. Rheological behavior of emulsions with 50% water cut at 70°C.

distance between droplets (derby length) brought about significant decrease in the collision intensity. At 25°C, SAL-0E50 droplets were able to break easier than those of SAL-2E50 due to lesser steric repulsion between the droplets. The collision impact was weaker and rupturing of the droplets might be dominant. SAL-1E50 maintained the same behavior as SAL-1E40, but required higher shearing force due to the closeness of the droplets at this level. The droplets became more agitated at elevated temperature and the collision intensity increased. Thus, SAL-2E50 droplets became easier to break and thereby assuming lesser viscosity profile than SAL-0E50.

4.3. Equal amount of emulsion phases

Figures 18–20 show the respective amount of water separation with time at three doses (50,000, 150,000 and 250,000 ppm) of SMES at 70°C. Demulsification obtained at 50000 ppm of SMES was faster in SAL-2E50 (100% water separation at 2 hours) followed by SAL-1E50

(100% water separation at 4 hours) and least in SAL-0E50 (100% at 96 hours) as shown in **Figure 14**. Increasing *SMES* dose to 150,000 ppm led to significant improvement in demulsification of SAL-1E50 and SAL-0E50 by shifting the time required to achieve 100% water separation to 2 hours and 6 hours respectively (**Figure 15**). Force of gravity dominated the demulsification process due to density difference. At 250000 ppm dose of *SMES*, 100% water separation was obtained in SAL-0E50 and SAL-2E50 within the first hour of testing but no significant increase in SAL-1E50 (**Figure 16**). Perhaps, the interfacial films of SAL-1E50 droplets became more elastic due to lower IFT and therefore, had quicker surface reconstruction after deformation.

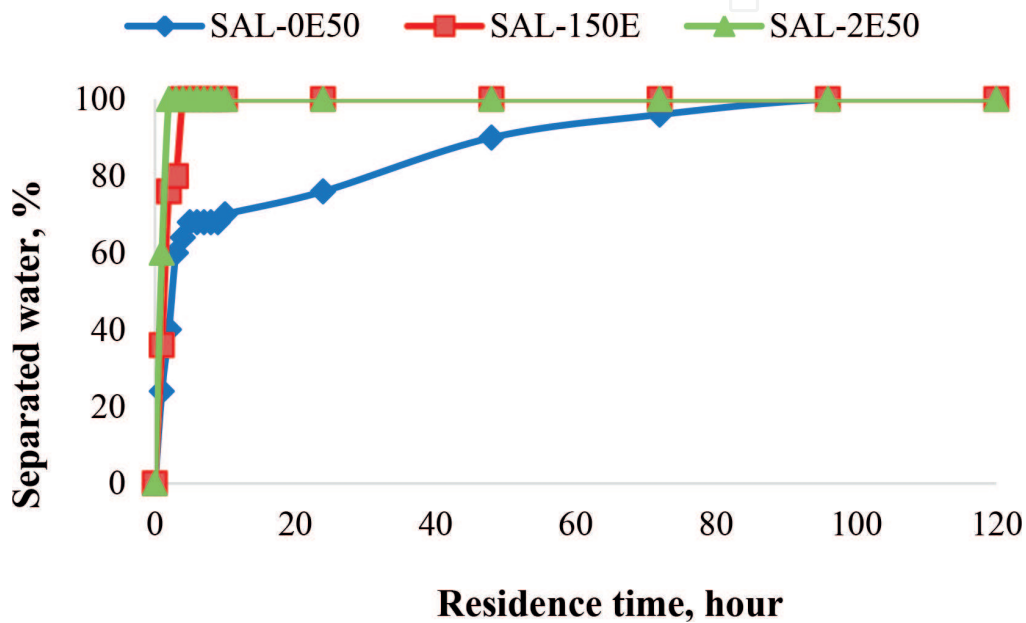


Figure 14. Phase separation at 50 g/L of *SMES* in emulsions with 50% water cut.

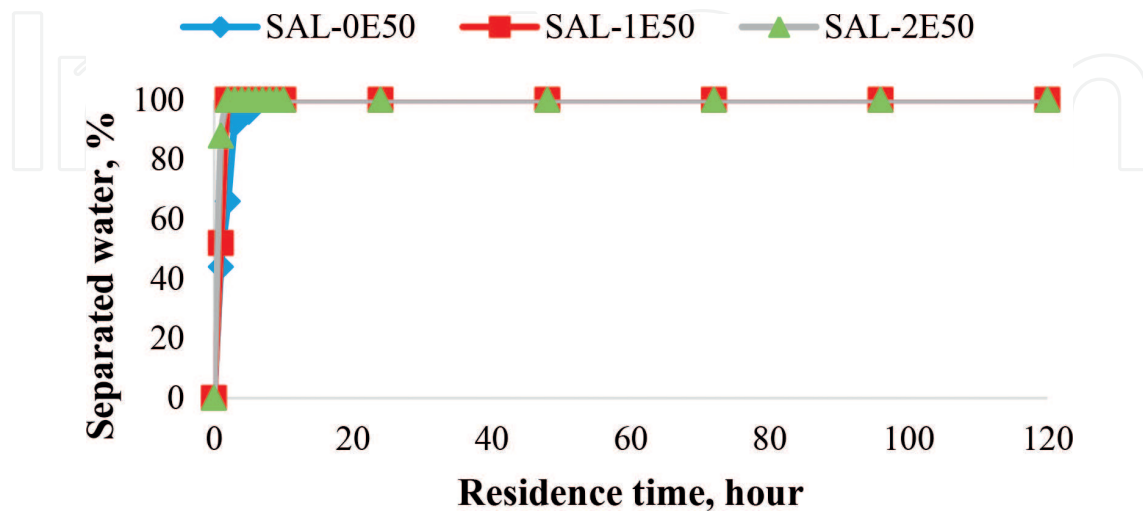


Figure 15. Phase separation at 150 g/L of *SMES* in emulsions with 50% water cut.

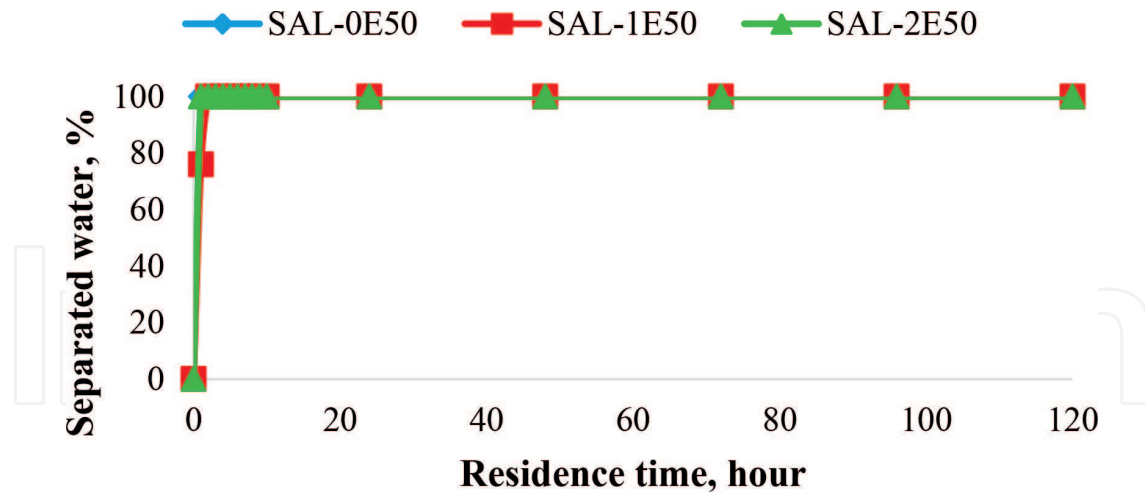


Figure 16. Phase separation at 250 g/L of *SMES* in emulsions with 50% water cut.

4.4. Demulsification of emulsions with lower water content

The respective phase separation profiles of SAL-0E40, SAL-1E40 and SAL-2E40 at 50,000, 150,000 and 250,000 ppm of *SMES* are shown in **Figures 21–23**. Obviously, the electrostatic repulsion in SAL-1E40 was higher at 50,000 ppm *SMES* dose due to dipole-dipole interactions between the salt ions present in SAL-1E40 and the Na^+ external to the emulsion droplets. This led to the least demulsification obtained in SAL-1E40 as shown in **Figure 17**. However, gravitational force was dominant in SAL-2E40 system and thereby leading to 100% water separation in 2 hours.

More *SMES* molecules as made available by 150,000 ppm dose improved resolution of the emulsions significantly (**Figure 18**). London van der Waals forces dominated the demulsification process in SAL-1E40 through the ability of the Na^+ external to droplets to overcome

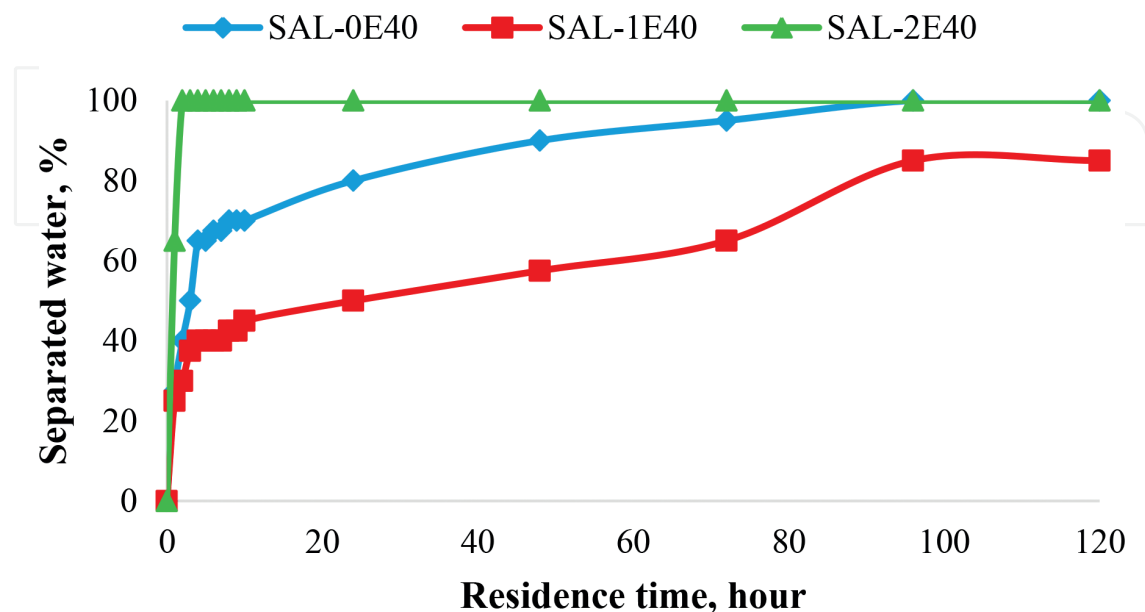


Figure 17. Phase separation at 50 g/L of *SMES* in emulsions with 40% water cut.

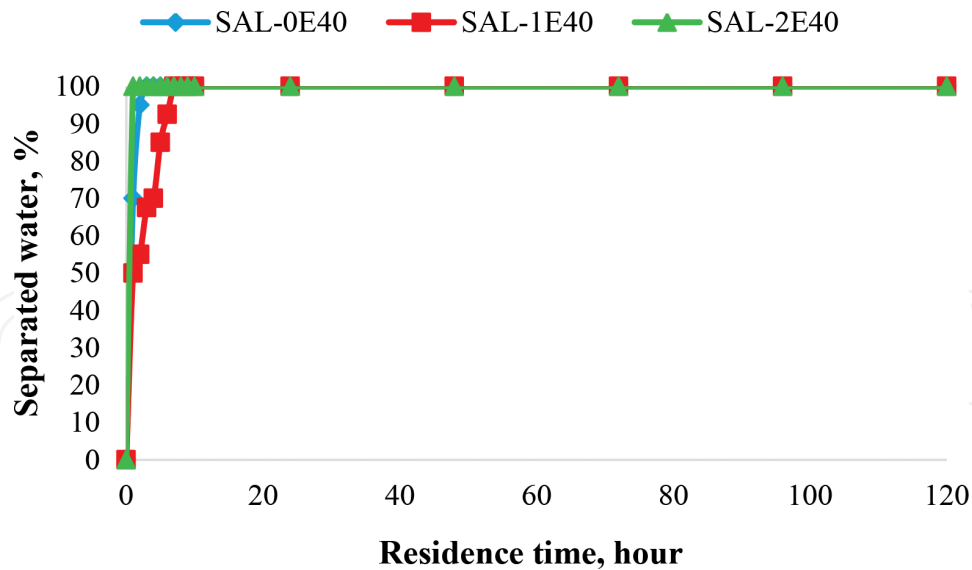


Figure 18. Phase separation at 150 g/L of SMES in emulsions with 40% water cut.

the repulsion presented by the ions present in the dispersed phase. Full phase separation occurred within 1 hour, 3 hours and 8 hours in SAL-2E40, SAL-0E40 and SAL-1E40 respectively. Subsequent increase in dosage to 250,000 ppm SMES led to 100% water separation within 1 hour in SAL-0E40 and 3 hours in SAL-1E40 (Figure 19).

The distance (Derby length) between the emulsions droplets was longer at 20% water cut. The droplets required adequate momentum to overcome the Derby length. Demulsification proceeded fastest in SAL-1E40 at 50000 ppm SMES (Figure 20) since it possessed highest momentum. Increase in dosage to 150,000 and 250,000 ppm brought about 100% phase separation in all the emulsions since adequate quantity of SMES was available to destabilize the droplets as depicted in Figures 21 and 22.

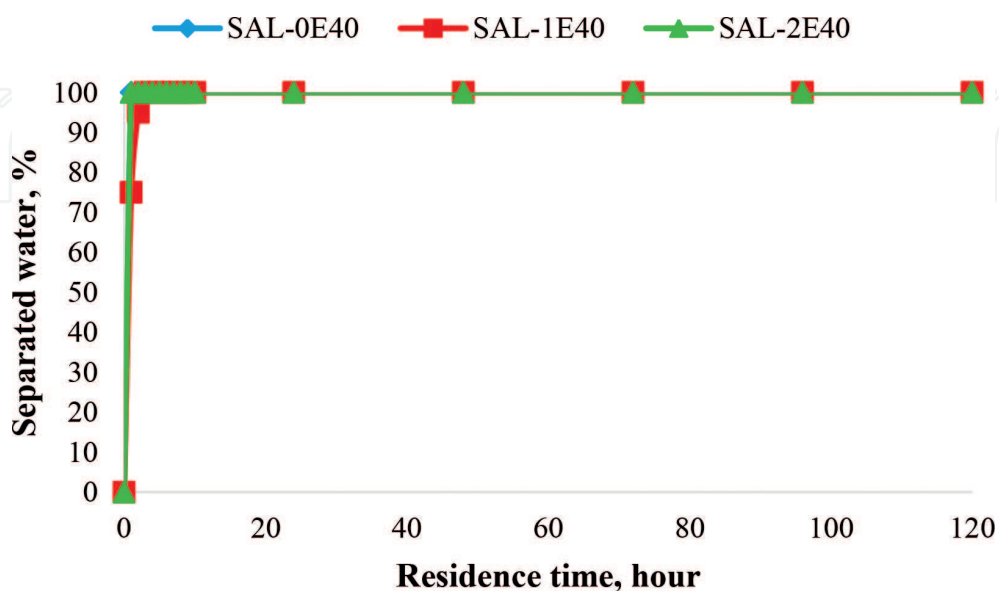


Figure 19. Phase separation at 250 g/L of SMES in emulsions with 40% water cut.

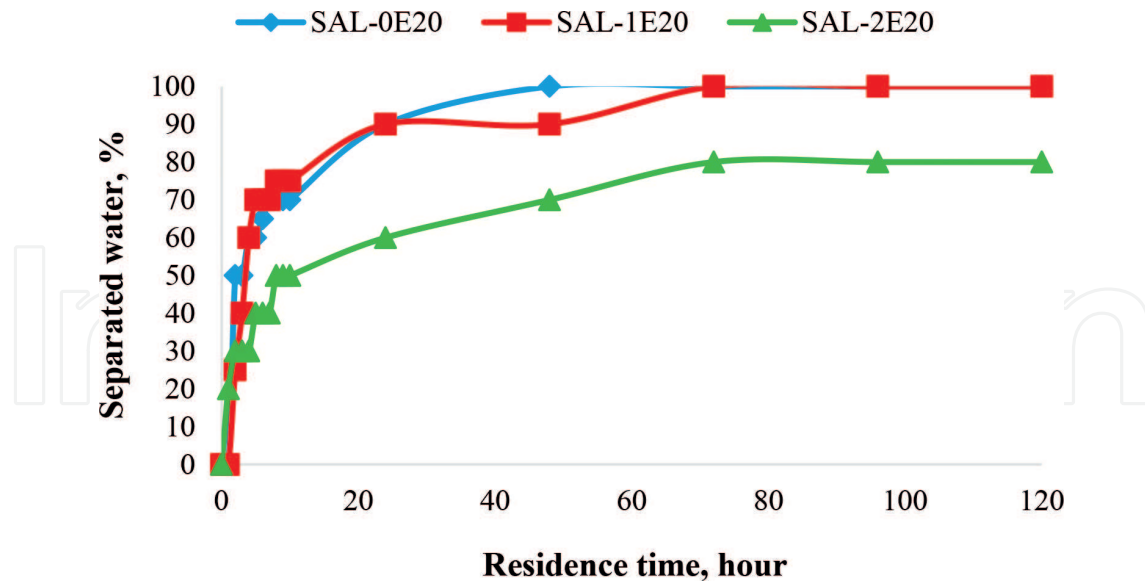


Figure 20. Phase separation at 50 g/L of *SMES* in emulsions with 20% water cut.

When added to emulsions, *SMES* dissociates into its anion and sodium salt action. It is adsorbed to the interface between the droplets and the crude oil with some preferential orientation according to the relative polarity of the interfacial film. Adsorption of surfactants is a dynamic occurrence which is prevented by another process that is responsible for surfactant transfer into the bulk phase. This phenomenon occurs rapidly. Consequently, equilibrium is attained after certain period depending on the concentration of the surfactant in the bulk phase. According to Salager [25], the free energy of the adsorbed molecules of surfactants is lower compared to the

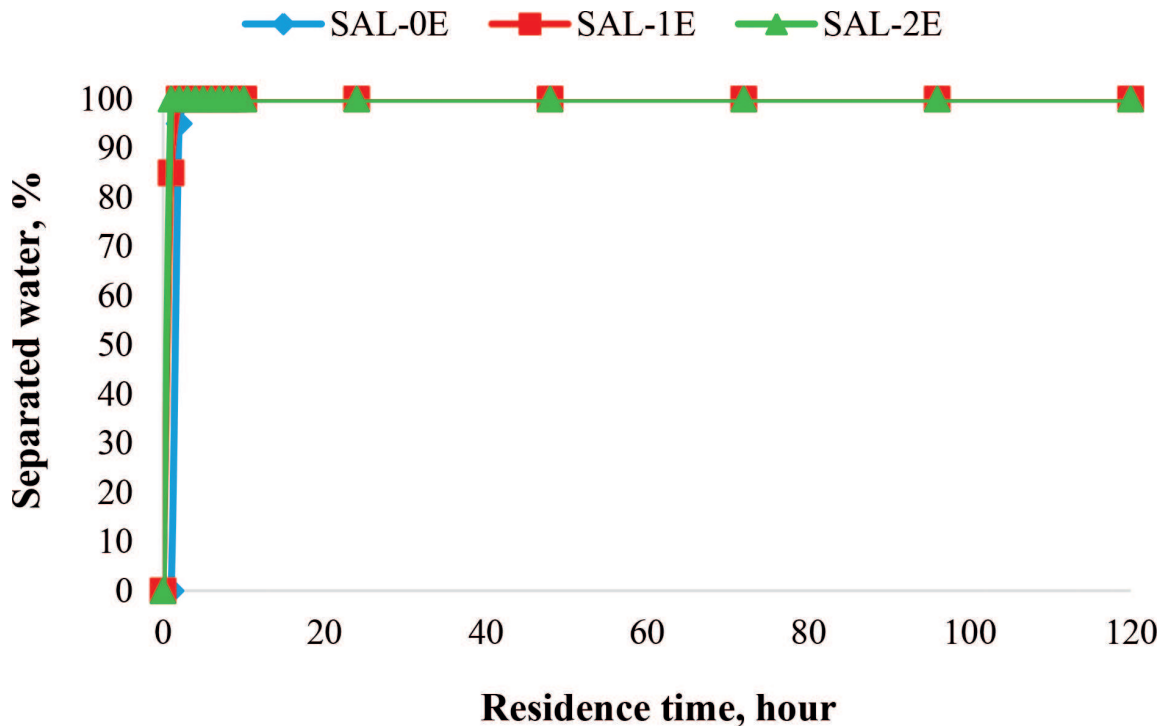


Figure 21. Phase separation at 150 g/L of *SMES* in emulsions with 20% water cut.

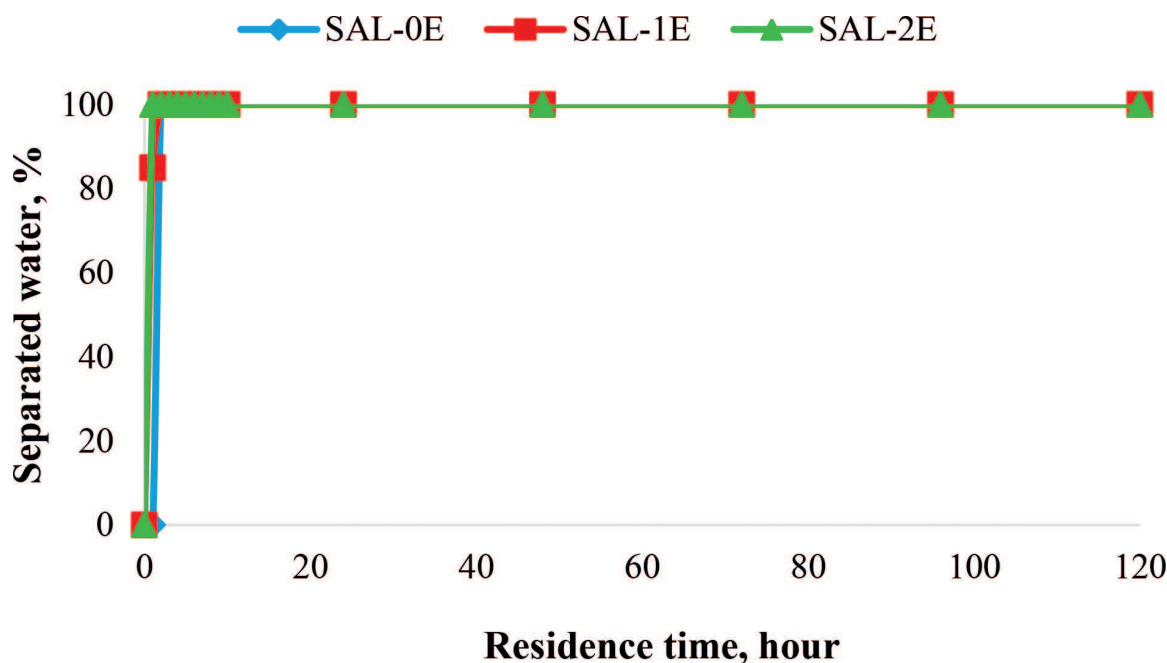


Figure 22. Phase separation at 250 g/L of *SMES* in emulsions with 20% water cut.

freer molecules in the bulk phase. Hence, the equilibrium is very much displaced towards the adsorbed state. Subsequently, a monolayer of the surfactant rapidly occupies the interface and the molecular arrangement of the surfactant depends its structural and geometrical properties.

In the presence of *SMES*, the cohesion between the droplets is substantially modified since this force action is very short, compared to the accumulating rate of the surfactant monolayer. The hydrophobic tail of the surfactant is adsorbed at the nonpolar phase leaving the hydrophilic head in the bulk phase. The anions are fixed to the interface, while the cations (Na^+) are subjected to random molecular motion. There is uniform distribution of the cations in the system and there exists a Coulomb attractive force between the adsorbed anions and the wandering cations. The Coulomb force prevents the cations from separating far away from the interface making them to form a layer located near to the interface. The stable dispersion experience in the emulsions with 20 percent water cut even in the presence of demulsifier was due to large Debye length that prevented the short-range forces from acting on the droplets. Increasing the concentration of electrolytes in the system will shorten the Debye length, especially the polyvalent electrolytes. Reducing the Debye length will lead to a shorter distance of potential overlapping, and thereby encouraging the short-range forces (cohesion and adhesion) to disrupt the emulsions. The steric repulsion among asphaltenes and resins (responsible for emulsion stability) is broken by this process.

5. Conclusion

There was a corresponding increase in pressure with water content and consequently, higher shearing force was required to make emulsions flow. Comparison of emulsion rheology profiles with shear rate shows the progressive increase in viscosity according to water content.

Collision impact, especially at elevated temperature was high enough to break the droplets but unable to destroy the interfacial film and, flocculation of the droplets was therefore impossible. The films encapsulating the emulsion droplets possess elastic properties that facilitated surface reconstruction of the interfacial films to compensate for “dimples” created after droplet deformation. Thus, it has been established that the interactions of the constituents of the crude oil system, the produced water system and the emulsion system play major roles in characterizing water-in-crude oil emulsions. The presence of interfacial films and the deviation of the emulsions from being Newtonian towards pseudo plastic behavior with respect to water cut and salinity suggest the breakage of emulsion droplets due to shear stress. Meanwhile, interfacial films possess surface reconstruction capability which ensures dimples coverage after collision impact. It was shown that the ease or difficulty with which droplets break depend largely on water cut and salinity. Hence, the stability of water-in-crude oil emulsions is related to the viscous force presented by the continuous phase, water cut and salinity.

Acknowledgements

The authors would like to thank the University Technology PETRONAS (UTP) for providing the grant used for this study and the permission to present the research findings.

Nomenclature

API	America petroleum institute
Ast	transformed resin content, %
BO	butylene oxide
BS 4708	method for determination of viscosity of transparent and opaque liquids (kinematic and dynamic viscosities)
BS	back scattering
BS & W	basic sediment and water
Ca	capillary number
CII	colloidal instability index
CRO	crude oil
ASTM D2500	standard test method for cloud point of petroleum product
ASTM D3279	standard test method for n-heptane insolubles
ASTM D445	standard test method for kinematic viscosity of transparent and opaque liquids (and calculation of dynamic viscosity)
ASTM D4928	standard test method for water in crude oils by Coulometric Karl Fischer Titration

ASTM D5002	standard test method for density and relative density of crude oils by digital density analyzer
ASTM D6591	standard test method for determination of aromatic hydrocarbon types in middle distillates-high performance liquid chromatography method with refractive index detection
ASTM D93	standard test methods for flash point by Pensky-Martens closed cup tester
DBSA	dodecylbenzene sulfonic acids
DCM	dichloromethane
DLVO	Derjaguin, Landau, Verwey and Overbeek
GCMS	gas chromatography mass spectrometry
HLB	hydrophilic-lipophilic balance
HPLC	high performance liquid chromatography
IFT	interfacial tension
K-F	Karl Fischer
MLS	multiple light scattering
NaCl	sodium chloride
NIR	near infrared
RI	refractive index
RID	refractive index detector
S&W	sediment and water
SAL-0	fresh water
SAL-0E20	20% SAL-0 cut-in-crude oil emulsion
SAL-0E40	40% SAL-0 cut-in-crude oil emulsion
SAL-0E50	50% SAL-0 cut-in-crude oil emulsion
SAL-1	brine solution (20000 ppm salinity)
SAL-1E20	20% SAL-1 cut-in-crude oil emulsion
SAL-1E40	40% SAL-1 cut-in-crude oil emulsion
SAL-1E50	50% SAL-1 cut-in-crude oil emulsion
SAL-2	brine solution (40000 ppm salinity)
SAL-2E20	20% SAL-2 cut-in-crude oil emulsion
SAL-2E40	40% SAL-2 cut-in-crude oil emulsion
SAL-2E50	50% SAL-2 cut-in-crude oil emulsion
SARA	saturates, aromatics, resins and asphaltenes

SG	specific gravity
SMES	sodium methyl ester sulfonate
UV	ultra-violet
VDWL	Van Der Waals London
Visc	untransformed natural logarithm of viscosity
Δp	pressure change
$\Delta \rho$	density difference
$\mu\text{S/cm}$	micro-Siemens per centimeter
1/k	extension of double layer
1/s	per second
Å	angstrom
Cl ⁻	chlorine ion
cP	centipoise
ϵ_0	relative permittivity
ϵ_r	permittivity of free space
g	asymmetry factor
g/cc, g/cm ³	gram per cubic centimeter
n	refractive index
Na ⁺	sodium ion
nm	nanometer
n_0	number of ions per unit volume of each type present in bulk solution
°C	degree Celsius
Qs	scattering efficiency
$R_a, R_{b,1}, R_{b,2}$	radius of curvature
T	absolute temperature
x	particle diameter
$\dot{\gamma}$	shear rate
Zi	valency of the ions
γ	interfacial tension
φ	concentration
ω	angular frequency
ℓ^*	photon transport mean free path

η	liquid dynamic viscosity
η_o	viscosity of a medium
κ_B	Boltzmann constant
ΣW	summation of water separation

Author details

Aliyu Adebayo Sulaimon* and Bamikole Joshua Adeyemi

*Address all correspondence to: aliyu.adebayor@utp.edu.my

Universiti Teknologi PETRONAS, Seri Iskandar, Perak, Malaysia

References

- [1] Kaiser A. Environmentally Friendly Emulsion Breakers: Vision or Reality? SPE International Symposium on Oilfield Chemistry. Woodlands, Texas, USA: Society of Petroleum Engineers Inc.; 2013
- [2] Oriji A, Appah D. Suitability of local demulsifier as an emulsion treating agent in oil and gas production. Paper SPE 162989 presented at the SPE Nigeria Annual international conference and exhibition (NAICE). Abuja, FCT, Nigeria; August 6-8 2012
- [3] Abdel-Aal H, Aggour M, Fahim M. Petroleum and Gas Field Processing. New York, BASEL: Marcel Dekker, Inc.; 2003
- [4] Kokal S. Crude Oil Emulsions. Petroleum Engineering Handbook – General Engineering. Vol. 1. Texas, USA: Society of Petroleum Engineers; 2006. pp. 533-570
- [5] Becker J. Crude Oil Waxes, Emulsions, and Asphaltenes. Tulsa, Oklahoma: PennWell Books; 1997
- [6] Othman A. Study on Emulsion Stability and Chemical Demulsification Characteristics. Bachelor Degree Thesis. Pahang: Universiti Malaysia Pahang; 2009
- [7] Stewart M, Arnold K. Emulsions and Oil Treating Equipment: Selection, Sizing and Troubleshooting. New York: Gulf Publishing, Elsevier; 2009
- [8] Zhou H, Dismuke K, Lett N, Penny G. Development of more environmentally friendly demulsifiers. In: I SPE 151852 Presented at the SPE International Symposium and Exhibition on Formation Damage Control. Kuala Lumpur, Malaysia: Society of Petroleum Engineers, Inc; February 15-17 2012
- [9] Koshelev V, Klimova L, Starikov V, Nizova S. New demulsifiers for petroleum preparation processes. Chemistry and Technology of Fuels and Oils. 2000;36(2)

- [10] Stout C, Nicksic S. Separation and gel permeation analysis of natural emulsion stabilizers. In: SPE 42nd Annual Fall Meeting. Vol. 243. Houston, Texas: American Institute of Mining, Metallurgical, and Petroleum Engineers, Inc; October 1-4 1967. pp. 253-259
- [11] Nghiem L, Hassam M, Nutakki R, George A. Efficient Modelling of Asphaltene Precipitation. Paper SPE 26642 presented at the SPE Annual Technical Conference and Exhibition. 1993;5:375-384
- [12] Sjoblom J, Urdahl O, Borve K, Mingyuan L, Saeten J, Christy A, et al. Stabilization and destabilization of water-in-crude oil emulsion from the Norwegian continental shelf. Correlation with model systems. *Advances in Colloid and Interface Science*. 1992;41:241-271
- [13] Fingas MF. Water-In-Oil Emulsions: Formation and Prediction. *Handbook of Oil Spill Science and Technology*. Toronto, Canada: John Wiley & Sons; 2014
- [14] Fingas M, Fieldhouse B. A review of knowledge on water-in-oil emulsions. *AMOP*. 2006:1-26
- [15] Tadros TF. *Emulsion Formation, Stability, and Rheology*. Applied Surfactants. Germany: Wiley-VCH Verlag GmbH; 2005
- [16] Eley D, Hey M, Symonds J. Emulsions of water in asphaltene-containing oils 1. Droplet size distribution and emulsification rates. *Colloids and Surfaces*. 1988;32:87-101
- [17] Gurkov TD, Basheva ES. Hydrodynamic Behaviour and Stability of Approaching Deformable Drops, "Encyclopedia of Surface and Colloid Science". New York: Marcel Dekker; 2002
- [18] Yarranton HW, Alboudwarej H, Jakher R. Investigation of Asphaltene association with vapor pressure Osmometry and interfacial tension measurements. *Industrial and Engineering Chemistry Research*. 2000;39(8):2916-2924
- [19] McLean JD, Kilpatrick PK. Effects of Asphaltene solvency on stability of water-in-crude-oil emulsions. *Journal of Colloid and Interface Science*. 1997;189:242-253
- [20] Al-Jarrah M, Al-Dujaih A. Characterization of some Iraqi asphalts II. New findings on physical nature of asphaltenes. *Fuel Science and Technology International*. 1989;7(1):69-88
- [21] Sztukowski D, Jafari M, Alboudwarej H, Yarranton H. Asphaltene self-association and water-in-hydrocarbon emulsions. *Journal of Colloid and Interface Science*. 2003; 265(1):179-186
- [22] Jamalluddin A, Nazarko T, Hills S, Fuhr B. Deasphalted oil: A natural asphaltene solvent. *Journal of SPE Production & Facilities*. Paper SPE 28994 presented at the 1995 SPE International Symposium on Oilfield Chemistry held in San Antonio, Feb. 14-17. Texas, USA: SPE International Symposium on Oilfield Chemistry; 1996
- [23] Sato T, Ruch R. *Stabilization of Colloidal Dispersions by Polymer Adsorption*. New York: Marcel Dekker Inc.; 1980

- [24] Claesson PM, Blomberg E, Poptoshev E. Surface Forces and Emulsion Stability. *Encyclopedic Handbook of Emulsion Technology*. New York: Marcel Dekker, Inc.; 2001; pp. 305-326
- [25] Salager JL. *Interfacial Phenomena in Dispersed Systems*. Laboratory of Formulation, Interfaces Rheology and Processes, FIRP Booklet # E120-N. Teaching Aid in Surfactant Science & Engineering. Universidad De Los Andes Facultad De Ingenieria Escuela De Ingenieria Quimica; 1994
- [26] Mackor EL, Van der Waals JH. The statistics of the adsorption of rod-shaped molecules in connection with the stability of certain colloidal dispersions. *Journal of Colloid Science*. 1952;**7**:535
- [27] Zapryanov Z, Malhotra AK, Aderangi N, Wasan DT. Emulsion stability: An analysis of the effects of bulk and interfacial properties on film mobility and drainage rate. *International Journal of Multiphase Flow*. 1983;**9**:105
- [28] Pichot R. *Stability and Characterisation of Emulsions in the presence of Colloidal Particles and Surfactants*. A PhD thesis submitted to the University of Birmingham, Department of Chemical Engineering, School of Engineering; 2010
- [29] Dukhin SS, Sjoblom J, Saether O. An experimental and theoretical approach to the dynamic behavior of emulsions, chap. 1. In: Sjoblom J, editor. *Emulsions and Emulsion Stability*. Boca Raton: CRC Press and Taylor & Francis Group; 2006
- [30] Miller DJ, Böhm R. Optical studies of coalescence in crude oil emulsions. *Journal of Petroleum Science and Engineering*. 1993;**9**(1):1-8
- [31] Elraies K, Tan M, Awang M, Saaid I. The synthesis and performance of sodium methyl ester sulfonate for enhanced oil recovery. *Petroleum Science and Technology*. 2010;**28**(17): 1799-1806
- [32] Razmah G, Salmiah A. Biodegradability and Ecotoxicity of palm stearin-based methyl Ester Sulphonates. *Journal of Oil Palm Research*. 2004;**16**(1):39-44
- [33] Masuda M, Odake H, Miura K, Oba K. Effects of 2-sulphonatofatty acid methyl ester (α -SFME) on aquatic organisms and activated sludge. *Journal of the American Oil Chemists' Society (Yukagaku)*. 1994;**43**(7):551-555
- [34] Sulaimon AA, Adeyemi BJ. Investigating the kinetics of water-in-crude oil emulsion stability. *ARNP Journal of Engineering and Applied Sciences*. 2015;**10**(16):7131-7136
- [35] Chugh KL. *ISC Chemistry: General and Physical Chemistry Part 1*. 9th ed. Kalyani Publishers; 2014
- [36] Aveyard R, Binks BP, Fletcher PDI. The resolution of water-in-crude oil emulsions by the addition of low molar mass demulsifiers. *Journal of Colloid and Interface Science*. 1990;**139**(1):128-138
- [37] Chhabra RP. *Non-Newtonian Fluids: An Introduction*. SERC School-Cum-Symposium on Rheology of Complex Fluids. India: Indian Institute of Technology Madras; Jan 1-4, 2010

